miRcorrNetPro: Unraveling Algorithmic Insights through Cross-Validation in Multi-Omics Integration for Comprehensive Data Analysis

Miray Unlu Yazici
Dept. of Bioengineering
Abdullah Gül University
Kayseri, Turkey
miray.unlu@agu.edu.tr

J. S. Marron
Dept. of Statistics and Operations Research
University of North Carolina
Chapel Hill, NC, USA
marron@unc.edu

Burcu Bakir-Gungor
Dept. of Computer Engineering
Abdullah Gul University
Kayseri, Turkey
burcu.gungor@agu.edu.tr

Malik Yousef
Dept. of Information Systems
Zefat Academic College
Zefat, Israel
malik.yousef@gmail

2023 IEEE International Conference on Bioinformatics and Biomedicine (BIBM) | 979-8-3503-3748-8/23/$31.00 ©2023 IEEE | DOI: 10.1109/BIBM58861.2023.10385425

***Abstract*—High throughput -omics technologies facilitate the investigation of regulatory mechanisms of complex diseases. Along this line, scientists develop promising tools and methods to extend our understanding at the molecular and functional levels. To this end, miRcorrNet tool performs integrative analysis of microRNA (miRNA) and gene expression profiles via machine learning (ML) approach to identify significant miRNA groups and their associated target genes. In this study, we propose miRcorrNetPro tool, which extends miRcorrNet by tracking group scoring, ranking and other information through the cross-validation iterations. Heatmap visualizations enable deep novel insights into the collective behavior of clusters of groups in cellular signaling and hence facilitate detection of potential biomarkers for the disease under investigation. Although miRcorrNetPro is designed as a generic tool, here we present our findings and potential miRNA biomarkers for Breast Cancer (BRCA). The miRcorrNetPro tool and all other supplementary files are available at https://github.com/Miray-Unlu/miRcorrNetPro.**

Keywords—Multi-omics Integration, microRNAs, Machine Learning, Breast Cancer

I. INTRODUCTION

Heterogeneity of cancer-like diseases is a key confound to understand the underlying characteristics of diseases with several etiologies and mechanisms. Immense amount of biological data generated with the advanced technology is analyzed with several promising tools and methods. These approaches have enabled the interpretation of the cellular mechanisms of heterogeneous diseases at multiple levels. Along this line, standard ML based tools initially focused on pure data-oriented approaches. The production of massive medical data sets at multiple layers have deflected these studies into integration-based procedures. Integration of multi-omics data and/or utilization of biological knowledge from several databases such as Gene Ontology [1], KEGG pathways [2] can improve the performance of the developed tools [3]. Some of these proposed methods are based on integrative analyses of gene expression and methylation data [4], copy number variations and mRNA expression [5]. From the ML perspective, supervised approaches such as Network-based integration of multi-omics data (NetICS) [6] and unsupervised methods such as Joint Non-negative Matrix Factorization (NMF) [7] have been introduced for feature selection in multi-omics data analysis. Most of the feature selection methods that are used in gene expression data analysis, exploit pure ML and statistics without considering deeper analyses of the features, interaction of the biomarkers and collective behavior of significant features.

The projected idea of this study is to bridge the interpretation gap between predictive biomarkers and their joint interaction in molecular and cellular processes, which may be causing the diseases. For this purpose, gene expression data and miRNA data are used to create groups following a scoring operation which selects informative groups with their associated genes. A machine learning model is constructed, and the information obtained via the iterations. Monte Carlo Cross-Validation (MCCV) is utilized for discovering distinct molecular patterns and new biomarkers within informative groups. Our tool enables classification of tumor/normal, disease subtypes, drug study groups and phenotypes of diseases through phenotypic similarity.

II. METHOD

Gene expression (mRNA-seq) and miRNA-seq data sets of BRCA are downloaded from the Cancer Genome Atlas data portal (https://portal.gdc.cancer.gov/). BRCA data sets are classified into two groups including 760 cases and 87 controls. There are 18571 genes and 217 miRNAs in this data set. Raw read counts of mRNAs and miRNAs are normalized with edgeR [8] based on TMM (Trimmed Mean of M-values) and RPM (Read Per Million) approaches, respectively. Normalized mRNA expression profiles are divided randomly into train and test splits. While 90% of the mRNA data including the normal and tumor samples is used for training of the classifier, performance of the model is evaluated on the 10% independent test data set.

The KNIME Analytics Platform [9], which is an open-source software, is used to develop the proposed miRcorrNetPro tool. The platform presents a wide range of operations for integration and analysis of large data sets. In this study, preprocessing of data sets, parameter settings, model fitting to a given data set, testing of the model and extended analyses are completed using the KNIME platform.

In our earlier study, we proposed miRcorrNet [10], which consists of 3 main components: grouping (G), scoring (S) and modeling (M). Similarly, several integrative tools, such as CogNet [11], PriPath [12], mirModuleNet [13], 3Mint [14] have used the Grouping-Scoring-Modeling (G-S-M) approach to incorporate biological knowledge associated with the

979-8-3503-3748-8/23/$31.00 ©2023 IEEE

diseases into gene expression data analysis. The main flowchart of miRcorrNetPro is illustrated in Fig. 1. Each of these components, implemented in our study can be summarized as follows: In the G component, the strength of association between each miRNA-mRNA pair (within the training data) is measured with Pearson correlation, using cor() function in R [15]. The pairs with correlation threshold lower than 0.8 are filtered out. The list of pairs given as an input in this step are grouped by miRNA names, and hence a set of groups are generated. Each group consists of a unique miRNA with single or multiple genes. Following that, the S component scores each of these highly associated groups in terms of accuracy measurement by using gene expression information. The groups are sorted by the score. In the M component, a Random Forest (RF) model is fitted to the given training data set. The test data set of gene expression is used for performance evaluation of the RF model. In the spirit of Monte Carlo Cross-Validation (MCCV), this process, based on a 90%-10% random split of the data, is repeated for 100 times. During these iterations, miRcorrNetPro tracks different levels of information for each group such as gene sets, scores and ranks. The co-occurrence patterns of BRCA associated groups are detected by a new P component proposed in this study. Furthermore, group features depending on the shared gene information among each pair of features are clustered and illustrated with hierarchical clustering approach. The output of miRcorrNetPro includes tables summarizing these quantities. Table 1 is an example of such tracked information. Additionally, miRcorrNetPro is a versatile tool that highlights important information from the tables using heatmap visualizations for detecting valuable biological knowledge. Another new component developed in miRcorrNetPro explains the behavior of the scores and ranks of the significant groups via visually representing the distribution of the frequencies of the groups over each rank.

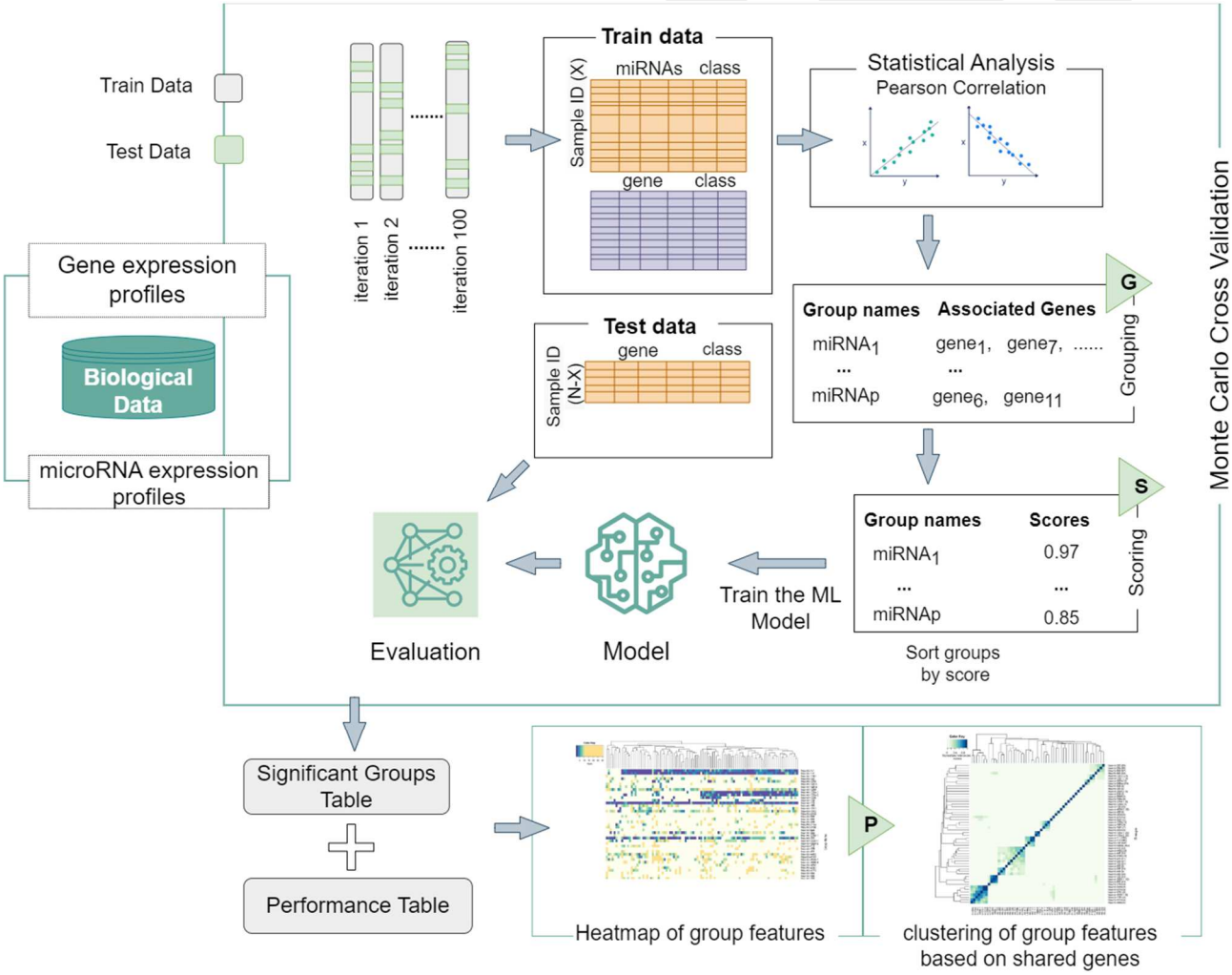

Fig 1. The workflow of mirCorrNetPro. The main components are Grouping (G), Scoring (S), Modelling (M) and Pattern identification (P). The output layer at the bottom shows significant groups and performance tables.

TABLE I. SIGNIFICANT GROUPS TABLE PROVIDING INFORMATION ABOUT THE FREQUENCY OF GROUPS, AVERAGE SCORE, AVERAGE RANK, NUMBER AND LISTS OF ASSOCIATED GENES

Group name	Frequency of Group	Average Score	Average Rank	# Associated Genes	Associated Genes	Iteration List	Rank List
hsa-mir-143	99	0.93	2.84	697	KLHL13, NFIX, EPHA3, ST8SIA1, …	0, 1, 2, 3, 4, 6, …	3, 1, 2, ….
hsa-mir-1-1	93	0.92	3.71	529	CCDC80, WFDC1, SMOC2,..	0, 1, 2, 3, 4, …	2, 3, 4, 4, 5, …
hsa-mir-1-2	93	0.92	3.3	585	CCDC80, WFDC1, SMOC2, XPNPEP2, …	0, 1, 2, 3, 4, …	1, 5, 4, …
hsa-mir-383	82	0.89	4.52	95	TAC1, CRTAC1, WIF1, …	0, 1, 2, 3, 4, …	2, 6, 3, 2, …
hsa-mir-548ba	79	0.83	7.8	384	METTL24, NNAT, KCNH2, PDZD4…	1, 2, 3, 4, 5, 6, …	5, 7, 5, 7, …
hsa-mir-1298	72	0.79	9.74	13	SCN11A, ASB12, DUSP2, DUSP26…	0, 1, 2, 5, 7, 8, …	5, 4, 9, …
hsa-mir-1912	69	0.79	10.01	9	SCN11A, ASB12, DUSP2, BRINP1, …	0, 1, 5, 7, 8, …	4, 7, 5, …
hsa-mir-133a-1	57	0.94	3.46	23	CLEC3B, PI16, RBM24, NRG2, …	1, 2, 3, 4, …	2, 1, 2, 4, …
hsa-mir-133a-2	56	0.94	3.34	20	CLEC3B, PI16, RASL11A, RBM24, NRG2, …	1, 2, 3, 4, 6, 7, …	7, 2, 1, 2, …
hsa-mir-4482	56	0.77	11.13	28	FCRL4, STAP1, CD79A, SLC24A4, MS4A1…	4, 6, 7, 8, 10, …	8, 9, 16, …

III. RESULTS & DISCUSSION

This section describes the results obtained with miRcorrNetPro on BRCA case and control data sets.

A. Identified Groups

Significant groups identified via co-occurrence analyses can provide a comprehensive knowledge about BRCA cellular mechanisms. Understanding the collective behavior and interconnection of the features can be utilized to elucidate the hidden layers of groups and/or genes within disease development processes. In this part of the study, we put effort into uncovering collective characteristics of the pairs of groups and clusters of groups over 100 iterations. For this purpose, significant players (groups) associated with the disease are identified and the relationships of the groups with related summaries are given in Table 1. In addition, deeper analysis about occurrence patterns of the groups over 100 iterations is illustrated as a heatmap in Fig. 2.

Table 1 summarizes the 10 most significant groups with relevant summary statistics. Frequency numbers show the appearance of groups over the 100 iterations. Averages of the scores and ranks of each group, over the iterations, calculated in the S component are given under the columns "Average Score" and "Average Rank" of this table respectively. "# Associated Genes" and "Associated Genes" are the number and the list of unique target genes of each group. "Iteration List" and "Rank List" columns present the lists of iterations in which each group is detected, together with its rank within that iteration. Higher scores demonstrate a better performance of the model for each group. In contrast, the lower the rank, the stronger the statistical significance of the group. All of the 10 groups listed in Table 1 appear in more than 50% of the total iterations, with the top 3 appearing very frequently. While the first 5 groups have several hundred associated genes, most of the others have far fewer. The groups hsa-miR-383, hsa-miR-133a-1 and hsa-miR-133a-2 have relatively high Average Scores, with a small number of associated genes.

B. Pattern detection in disease associated groups using the proposed P component

Next, we put effort into uncovering collective characteristics of the pairs of groups and clusters of groups over the 100 iterations, beyond the information displayed in Table 1. In addition, deeper analysis about occurrence patterns of the groups over 100 iterations is illustrated as a heatmap in Fig. 2. Significant groups identified via co-occurrence analyses can provide comprehensive insights about BRCA cellular mechanisms. Understanding the collective behavior and interconnection of the features can be utilized to elucidate the hidden layers of groups and/or genes within disease development processes. The occurrence patterns of the groups with rank and iteration information displayed in Table 1, together with all other groups that appeared in at least 5 iterations, are illustrated in Fig. 2. For enhanced visual understanding, iterations (columns) with similar patterns are placed near each other in the heatmap by

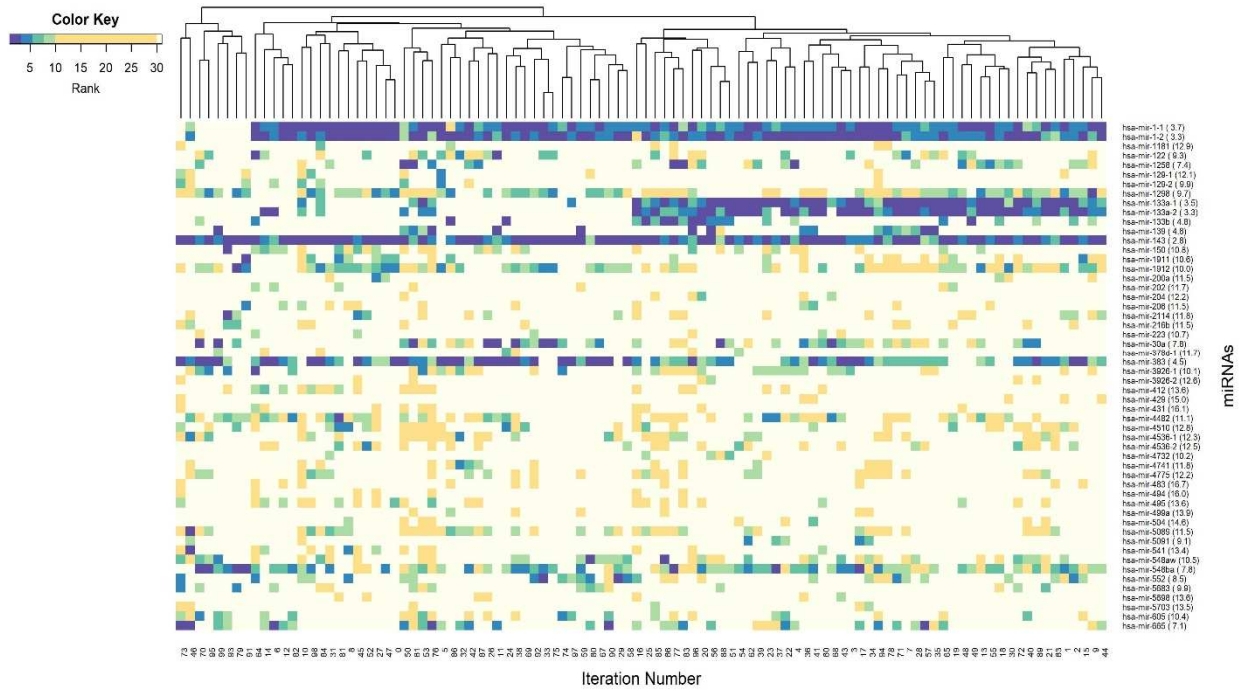

Fig 2. Heatmap of group features with rank information for each split. The co-occurrence patterns of groups are shown over splits. The rank of each group is presented with a sequential color scheme where dark blue colors represent the top ranks. Non-detected groups are displayed with light yellow color for corresponding splits.

using hierarchical clustering with average-linkage based on Euclidean distances.

The dendrogram of this clustering appears on the top. While the top ranked features (groups) are displayed with dark blue colors, non-detected groups for corresponding iterations are indicated with light yellow colors. In this context, groups with dark blue patterns denote the strongly significant players over the splits. The top three significant (dominant) groups (i.e., hsa-miR-143, hsa-miR-1-1, hsa-miR-1-2) appear in almost all iterations with an average rank of 2.84, 3.71 and 3.3, respectively.

Furthermore, the groups hsa-miR-133a-1, hsa-miR-133a-2 and hsa-miR-133b appear in approximately 50% of the total iterations, as shown on the right side of Fig. 2 with the dominant groups. More in-depth investigation of the occurrence behavior of these groups enables elucidation of the potential role of particular groups in cellular signaling in BRCA.

C. Performance Results of miRcorrNetPro

Table 2 presents the performance table of miRcorrNetPro for classifying BRCA using 100 fold MCVV. The symbol '±' denotes the standard deviation of the mean. Summary statistics in this table are improved with assembly of more cumulative groups (from top to bottom in the table). Cumulative group 9 generates best performance metrics. The following cumulative group (i.e., group #10) does not increase the performance of the model. Classification performance was quite strong with over 95% accuracy and 0.99 area under the curve (AUC) metrics.

D. Clustering of group features based on the shared genes

We have described important features based on the iteration and rank information so far. Fig. 3 aims to lay the groundwork for a better understanding and distinct collective interpretation of significant features depending on how genes are shared between the significant groups which are shown in Fig. 2. Initially, a two-dimensional similarity matrix is constructed. This matrix encodes the normalized number of intersected genes of each pairwise group with the total (union) number of genes in the groups. A heatmap visualization of that square matrix is shown in Fig. 3, where the x-axes and y-axes are labeled by the group names.

TABLE II. PERFORMANCE TABLE OF MIRCORRNETPRO FOR BRCA CLASSIFICATION USING 100-FOLD MCVV

Cumulative Group #	Accuracy	Specificity	Sensitivity	Area Under Curve
1	0.96	0.97	0.93	0.99
2	0.96	0.97	0.94	0.99
3	0.96	0.97	0.94	0.99
4	0.96	0.97	0.94	1
5	0.96	0.97	0.95	1
6	0.96	0.97	0.95	1
7	0.96	0.98	0.93	1
8	0.97	0.99	0.94	1
9	0.97	0.98	0.95	1
10	0.94	0.94	0.93	0.99

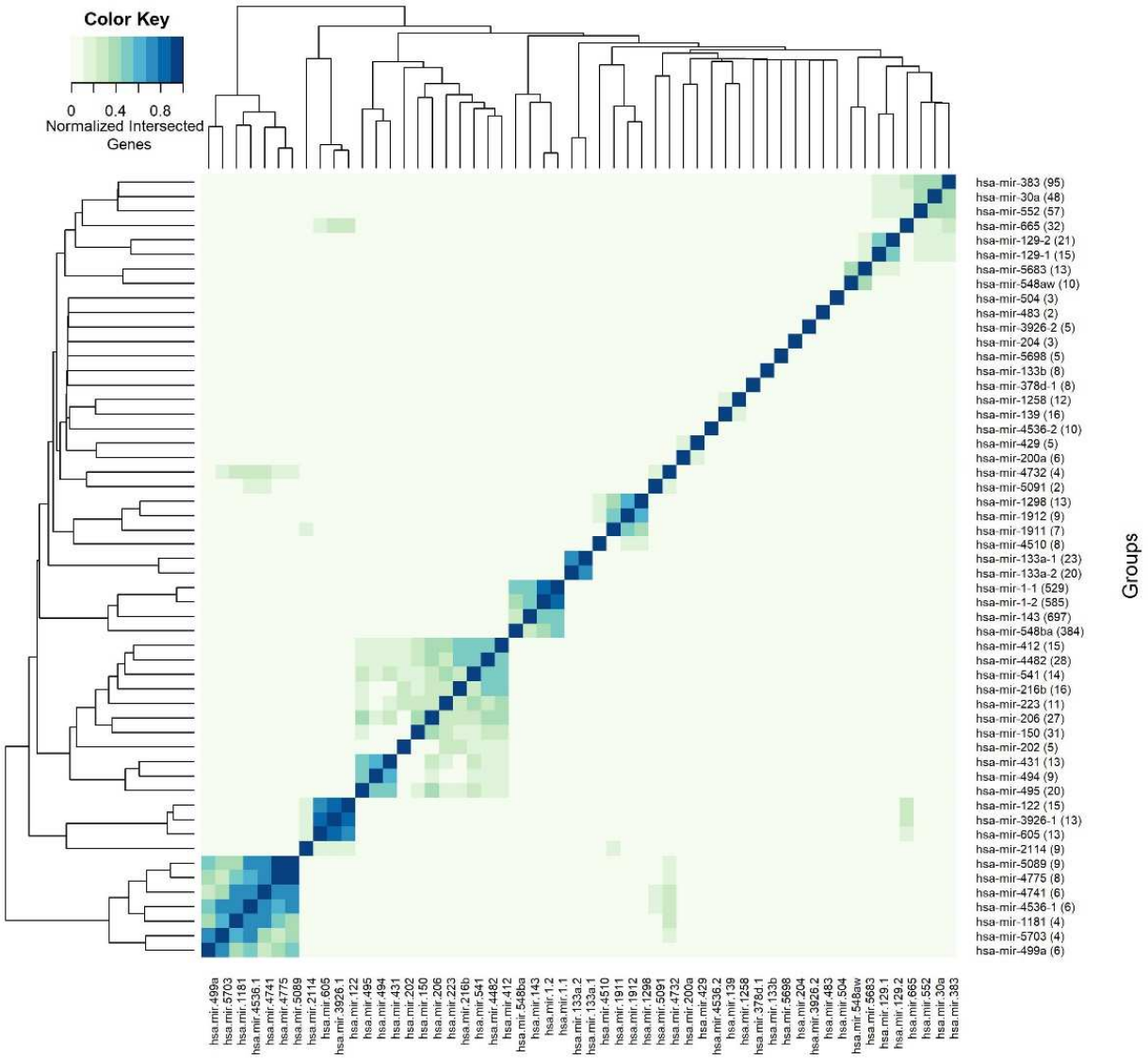

Fig 3. Heatmap and dendrograms showing clustering of group features depending on shared genes among each pair of features. Normalized intersected gene numbers of each pair of groups are encoded as colors. Scaling the normalized gene number from lower to higher in the range of (0,1). The number of unique gene sets of each group is given in parentheses after the group names.

Fig. 3 scales the normalized gene information in the range of 0 to 1, where darker color indicates higher number of normalized shared genes. Once again, for enhanced visualization, both the columns and rows are hierarchically clustered. The purpose of this analysis is not merely elucidation of hidden relationships between pairs of groups, but also unveiling the collective characteristics of clusters of groups. Fig. 3 shows a number of apparently interesting blocks (square packs colored by normalized intersected gene information) along the main diagonal. The groups hsa-miR133a-1 and hsa-miR-133a-2 in the block near the center of the heatmap are very strongly associated, which is consistent withtheir very similar occurrence patterns seen in Fig. 2. Another block consisting of the groups hsa-miR-1-1, hsa-miR-1-2, hsa-miR-143 and hsa-miR-548ba, also have very similar iteration patterns in Fig. 2. The miR-1/133a family is seen to be highly conserved (across species) with the clusters of miR-1-1/miR-133a-2 and miR1-2/miR-133a-1, located in the intronic regions of the genes C20orf166 and M1B1 on chromosomes 20 and 18, respectively. In Fig. 3, the bottom left block suggests a strong cluster including 7 groups; and the previous cluster consists of 3 conserved groups with bigger gene sets. The miR-206 and 133b are clustered together in the gene IL-17a on chromosome 6. Several studies reported the significant downregulation of these clusters in several cancer types. The most frequently appeared miRNAs, i.e. miR-143-5p, miR-1-1, miR-1-2 are downregulated in BRCA, which is associated with cell proliferation and migration [16]. It is reported [17] that the downregulation of hsa-miR-383, another frequently appeared miRNA, in BRCA tissues. This is consistent with our findings on the importance of identified groups and miRNA clusters for the classification of the given BRCA tumor and normal samples.

When the groups are evaluated in terms of their hierarchical clustering in Fig. 3, the distance between the groups hsa-miR-

133a-1, hsa-miR-133a-2 and hsa-miR-1-1, hsa-miR-1-2 are small, considering a great difference in the number of gene sets. It supports the idea that the size of the gene list may also influence the clustering results. In addition, the positioning of these groups next to each other in the hierarchical clustering may underpin the idea of "groups in close proximity (in the heatmap) working together", when the functions of the clusters miR-1-1/miR-133a-2 and miR1-2/miR-133a-1 are taken into account.

From a gene centric point of view, miRcorrNetPro detected the most frequently appeared genes across the significant groups: HPSE2, RASL12, DACT3. A literature search for these genes has revealed that the downregulation of the gene HSPE2 (Heparanase 2) in BRCA affects cell growth and metastasis [18]. RASL12 (RAS Like Family 12) is identified as another potential gene which is a member of the

RAS subfamily of small GTPases. Considering the tumor suppression role of many members of this family, RASL12 has a promising role in growth control and migration of cancer cells [19]. It is reported that DACT3 acts as a negative regulator in Wnt/beta-catenin signaling in colorectal cancer [20]. From groups and their associated genes perspective, experimentally validated interactions of miRNAs and target genes are searched in the database miRTarBase [21].

The 42 genes such as PDE5A, NFIC, LMOD3, SYT11, THRA, DNAJC18 (sorted from most frequently appeared to less) targeted by hsa-miR-143 in our analysis, are also experimentally supported by miRTarBase. In order to understand the dysregulation mechanisms of BRCA, over-representation analysis is carried out using KEGG pathways. Among the significantly enriched pathways ($p < 0.05$) that are identified in our analysis, Platelet Activation (hsa04611) and cAMP signaling (hsa04024) are known as critical processes in cell migration and motility of cancer cells in BRCA [22]; [23]. Another most frequently appearing miRNA, hsa-miR-383 is associated with 28 genes including DNAJC18, GAS7, OSBPL10, PARVA, SCN2B, BCL10, BVES, CNNM1 (according to the frequency in decreasing order). These genes are also experimentally shown to be related with BRCA in the miRTarBase database. The signaling pathways cGMP-PKG (hsa04022) and JAK-STAT (hsa04630), which have essential role in metastasis of BRCA [24], [25], are found to be functionally enriched in our analysis for the list of genes targeted by hsa-miR-383.

IV. Conclusion

The objective of this study is to provide a deeper insight into the interaction and collective behavior of the microRNAs and mRNA expression levels, utilizing group and ranking information obtained within the cross-validation steps of the proposed ML model. A novel P component is designed and integrated into the G-S-M approach. Hence, miRcorrNetPro tool is developed for pattern detection and clustering of groups associated with the disease under investigation. Here we have presented our findings using miRcorrNetPro on BRCA data set, downloaded from TCGA. Conventional ML methods utilize cross-validation techniques for performance evaluation. Though, the ranks and scores obtained within MCCV iterations are used by miRcorrNetPro. Thus, we facilitate the identification and association of potential biomarkers by performing grouping and scoring of the features used within the supervised machine learning models. The hidden patterns of groups and clusters associated with the disease under investigation are attained via the G-S-M-P approach. As a result, this approach provides a comprehensive view of cell signaling at the molecular level in heterogeneous diseases through integration of -omics data sets.

References

[1] The Gene Ontology Consortium, "The Gene Ontology Resource: 20 years and still GOing strong," Nucleic Acids Res., vol. 47, no. D1, pp. D330–D338, Jan. 2019, doi: 10.1093/nar/gky1055..

[2] M. Kanehisa, M. Furumichi, M. Tanabe, Y. Sato, and K. Morishima, "KEGG: new perspectives on genomes, pathways, diseases and drugs," Nucleic Acids Res., vol. 45, no. D1, pp. D353–D361, Jan. 2017, doi: 10.1093/nar/gkw1092.

[3] C. Perscheid, "Integrative biomarker detection on high-dimensional gene expression data sets: a survey on prior knowledge approaches," Brief. Bioinform., vol. 22, no. 3, p. bbaa151, May 2021, doi: 10.1093/bib/bbaa151.

[4] Z. Gong, J. Chen, J. Wang, S. Liu, C. B. Ambrosone, and M. J. Higgins, "Differential methylation and expression patterns of microRNAs in relation to breast cancer subtypes among American women of African and European ancestry," PLOS ONE, vol. 16, no. 3, p. e0249229, Mar. 2021, doi: 10.1371/journal.pone.0249229.

[5] Y. Xia, C. Fan, K. A. Hoadley, J. S. Parker, and C. M. Perou, "Genetic determinants of the molecular portraits of epithelial cancers," Nat. Commun., vol. 10, no. 1, p. 5666, Dec. 2019, doi: 10.1038/s41467-019-13588-2.

[6] C. Dimitrakopoulos et al., "Network-based integration of multi-omics data for prioritizing cancer genes," Bioinformatics, vol. 34, no. 14, pp. 2441–2448, Jul. 2018, doi: 10.1093/bioinformatics/bty148.

[7] S. Zhang, C.-C. Liu, W. Li, H. Shen, P. W. Laird, and X. J. Zhou, "Discovery of multi-dimensional modules by integrative analysis of cancer genomic data," Nucleic Acids Res., vol. 40, no. 19, pp. 9379–9391, Oct. 2012, doi: 10.1093/nar/gks725.

[8] M. D. Robinson, D. J. McCarthy, and G. K. Smyth, "edgeR: a Bioconductor package for differential expression analysis of digital gene expression data," Bioinformatics, vol. 26, no. 1, pp. 139–140, Jan. 2010, doi: 10.1093/bioinformatics/btp616.

[9] M. R. Berthold et al., "KNIME - the Konstanz information miner: version 2.0 and beyond," ACM SIGKDD Explor. Newsl., vol. 11, no. 1, pp. 26–31, Nov. 2009, doi: 10.1145/1656274.1656280.

[10] M. Yousef, G. Goy, R. Mitra, C. M. Eischen, A. Jabeer, and B. Bakir-Gungor, "miRcorrNet: machine learning-based integration of miRNA and mRNA expression profiles, combined with feature grouping and ranking," PeerJ, vol. 9, p. e11458, May 2021, doi: 10.7717/peerj.11458.

[11] M. Yousef, E. Ülgen, and O. Uğur Sezerman, "CogNet: classification of gene expression data based on ranked active-subnetwork-oriented KEGG pathway enrichment analysis," PeerJ Comput. Sci., vol. 7, p. e336, Feb. 2021, doi: 10.7717/peerj-cs.336.

[12] M. Yousef, F. Ozdemir, A. Jaaber, J. Allmer, and B. Bakir-Gungor, "PriPath: Identifying Dysregulated Pathways from Differential Gene Expression via Grouping, Scoring and Modeling with an Embedded Machine Learning Approach," In Review, preprint, Apr. 2022. doi: 10.21203/rs.3.rs-1449467/v1.

[13] M. Yousef, G. Goy, and B. Bakir-Gungor, "miRModuleNet: Detecting miRNA-mRNA Regulatory Modules," Front. Genet., vol. 13, p. 767455, Apr. 2022, doi: 10.3389/fgene.2022.767455.

[14] M. Unlu Yazici, J. S. Marron, B. Bakir-Gungor, F. Zou, and M. Yousef, "Invention of 3Mint for feature grouping and scoring in multi-omics," Front. Genet., vol. 14, p. 1093326, Mar. 2023, doi: 10.3389/fgene.2023.1093326.

[15] R Core Team, "R: A Language and Environment for Statistical Computing." Vienna, Austria, 2021. [Online]. Available: https://www.r-project.org/

[16] J. Peng et al., "Upregulation of microRNA-1 inhibits proliferation and metastasis of breast cancer," Mol. Med. Rep., vol. 22, no. 1, pp. 454–464, May 2020, doi: 10.3892/mmr.2020.11111.

[17] J. Zhang, X. Kong, Q. Shi, and B. Zhao, "MicroRNA-383-5p acts as a potential prognostic biomarker and an inhibitor of tumor cell proliferation, migration, and invasion in breast cancer," Cancer Biomark., vol. 27, no. 4, pp. 423–432, Mar. 2020, doi: 10.3233/CBM-190704.

[18] X. Huang et al., "Heparanase Promotes Syndecan-1 Expression to Mediate Fibrillar Collagen and Mammographic Density in Human Breast Tissue Cultured ex vivo," Front. Cell Dev. Biol., vol. 8, p. 599, Jul. 2020, doi: 10.3389/fcell.2020.00599.

[19] C. Lo Nigro et al., "NT5E CpG island methylation is a favourable breast cancer biomarker," Br. J. Cancer, vol. 107, no. 1, pp. 75–83, Jun. 2012, doi: 10.1038/bjc.2012.212.
[20] X. Jiang et al., "DACT3 Is an Epigenetic Regulator of Wnt/β-Catenin Signaling in Colorectal Cancer and Is a Therapeutic Target of Histone Modifications," Cancer Cell, vol. 13, no. 6, pp. 529–541, Jun. 2008, doi: 10.1016/j.ccr.2008.04.019.
[21] H.-Y. Huang et al., "miRTarBase 2020: updates to the experimentally validated microRNA–target interaction database," Nucleic Acids Res., p. gkz896, Oct. 2019, doi: 10.1093/nar/gkz896.
[22] A. Braun, H.-J. Anders, T. Gudermann, and E. Mammadova-Bach, "Platelet-Cancer Interplay: Molecular Mechanisms and New Therapeutic Avenues," Front. Oncol., vol. 11, p. 665534, Jul. 2021, doi: 10.3389/fonc.2021.665534.
[23] M. B. Ahmed, A. A. A. Alghamdi, S. U. Islam, J.-S. Lee, and Y.-S. Lee, "cAMP Signaling in Cancer: A PKA-CREB and EPAC-Centric Approach," Cells, vol. 11, no. 13, p. 2020, Jun. 2022, doi: 10.3390/cells11132020.
[24] R. Schwappacher, H. Rangaswami, J. Su-Yuo, A. Hassad, R. Spitler, and D. E. Casteel, "cGMP-dependent Protein Kinase Iβ Regulates Breast Cancer Cell Migration and Invasion via a Novel Interaction with the Actin/Myosin-associated Protein Caldesmon," J. Cell Sci., p. jcs.118190, Jan. 2013, doi: 10.1242/jcs.118190.
[25] F. Shao, X. Pang, and G. H. Baeg, "Targeting the JAK/STAT Signaling Pathway for Breast Cancer," Curr. Med. Chem., vol. 28, no. 25, pp. 5137–5151, Aug. 2021, doi: 10.2174/0929867328666201207202012.